ACS APPLIED MATERIALS & INTERFACES

Research Article

www.acsami.org

Circumventing the Mechanochemical Origins of Strength Loss in the Synthesis of Hierarchical Carbon Fibers

Stephen A. Steiner, III,* Richard Li, and Brian L. Wardle

Department of Aeronautics and Astronautics, Massachusetts Institute of Technology, 77 Massachusetts Avenue, Cambridge, Massachusetts, United States 02139

Supporting Information

ABSTRACT: Hierarchical carbon fibers (CFs) sheathed with radial arrays of carbon nanotubes (CNTs) are promising candidates for improving the intra- and interlaminar properties of advanced fiber-reinforced composites (e.g., graphite/epoxy) and for high-surface-area electrodes for battery and supercapacitor architectures. While CVD growth of CNTs on CFs has been previously shown to improve the apparent shear strength between fibers and polymer matrices (up to 60%), this has to date been achieved only at the expense of significant reductions in tensile strength (~30−50%) and stiffness (~10−20%) of the underlying fiber. Here we demonstrate two approaches for growing aligned and unaligned CNTs on CFs that enable preservation of fiber strength and stiffness. We observe that CVD-induced reduction of fiber strength and stiffness is primarily attributable to mechanochemical reorganization of the underlying fiber when heated untensioned above ~550 °C in both hydrocarbon-containing and inert atmospheres. We show that tensioning fibers to ≥12% of tensile strength during CVD enables aligned CNT growth while simultaneously preserving fiber strength and stiffness even at growth temperatures >700 °C. We also show that CNT growth employing CO_2/acetylene at 480 °C without tensioning—below the identified critical strength-loss temperature—preserves fiber strength. These results highlight previously unidentified mechanisms underlying synthesis of hierarchical CFs and demonstrate scalable, facile methods for doing so.

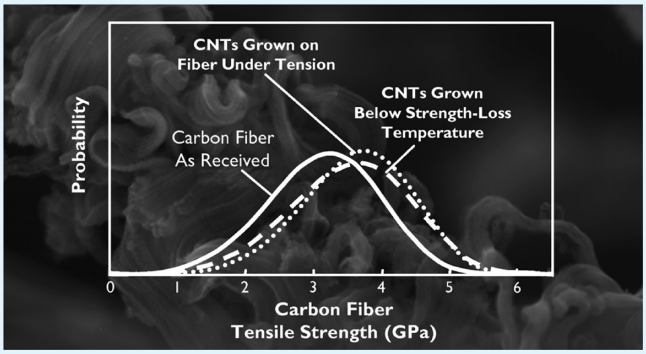

KEYWORDS: *carbon nanotubes, hierarchical fibers, carbon fiber, mechanochemistry, noncovalent functionalization*

1. INTRODUCTION

Advanced filamentary composites are an important class of structural materials with mass-specific strength and stiffness properties superior to metal alloys. Composites are critical for production of fuel-efficient long-haul aircraft, energy-efficient electric cars and trucks, large-scale wind turbines, and cost-effective spacecraft.[1] Important examples include fiberglass/polyurethane (amorphous glass fibers bonded by polyurethane resin), carbon/carbon (carbon fibers bonded by an amorphous pyrolyzed carbon matrix), and carbon fiber-reinforced plastics (CFRPs) such as graphite/epoxy (carbon fibers bonded by epoxy resin). Graphite/epoxy serves an especially important role in aerospace engineering as a functional materials platform because the macroscopic properties of graphite/epoxy laminates (e.g., coefficients of thermal expansion, mechanical responses) can be nonisotropically tailored through configuration of laminate lay-up and appropriate selection of matrix, thereby enabling production of sophisticated aeroelastic and zero-CTE structures of great technological value.

There are many situations in which current composite architectures underperform metal alloys (e.g., shear loading), however, and thus cannot be leveraged for their weight-saving or multifunctional advantages. Additionally, in applications such as aircraft lightning strike protection and wind turbines where structures must conduct electricity, the high electrical resistivity of graphite/epoxy often calls for inclusion of additional conductive elements (e.g., copper or aluminum mesh) that add additional weight.[2] The origins of these various performance limitations can be traced to the microscopic interstices of matrix (e.g., polymers such as epoxy) that join fibers and plies together in the laminate, which are where ply delamination, fracture propagation, and electrical resistance arise. One way to address these limitations is to reinforce such interstices with nanostructured fibers in a fashion analogous to how the carbon microfibers reinforce the macroscopic volumes of epoxy in the bulk composite. In typical fiber-reinforced plastic (FRP) composites, these expanses, typically on the order of 100 to 1000 nm across, provide more than ample space for inclusion of a plurality of nanoscale objects. Nanostructured materials introduced in this way could thus enable installation of both interlaminar (between plies) and intralaminar (among tows and fibers in a ply) reinforcement of the composite at the nanoscale,

Received: February 19, 2013
Accepted: April 24, 2013
Published: April 24, 2013

   dx.doi.org/10.1021/am4006385 | ACS Appl. Mater. Interfaces 2013, 5, 4892−4903

thereby leaving the microfiber architecture of the laminate undisturbed.

A number of different strategies for introducing nanoscale fibers into composite architectures have been attempted, including shear mixing of CNTs into matrix materials,[3−6] placement of unaligned[7−10] and aligned[11] CNTs at the interface of plies, and direct growth of CNTs on ceramic cloths[12] but have to date resulted in only marginal reported improvements in mechanical properties in both nanocomposites and microfiber-reinforced composites (see Shaffer et al. for a review of recent work in this area[13]). Nanoengineered hierarchical fiber architectures are a promising alternative approach for improving fracture toughness, interlaminar and intralaminar strength, and wear resistance of advanced fiber composites such as graphite/epoxy and carbon/carbon.[13] In recent years, hierarchical fiber architectures have been shown to result in improvements in the fracture toughness, interlaminar shear strength, and bearing properties in alumina/epoxy composites.[14−16] Wardle et al. showed that using a high catalyst density for CVD growth of CNTs on alumina fibers results in aligned CNT arrays ("forests")[15,17] that facilitate capillarity-driven wetting[18] of resins into the microfiber architecture and enable the toughness and strength enhancement observed in alumina/epoxy composites (so-called alumina fuzzy-fiber-reinforced plastics or "alumina FFRPs").[14] Incorporation of aligned CNTs onto fiber surfaces has also been shown to be an advantageous morphological feature for enhancement of nonmechanical properties.[14−17,19,20] Additionally, a scale effect in fracture toughness has been identified via simple closed-form bridging models,[20] and has been corroborated via interlaminar toughness testing of aligned CNT-reinforced alumina/epoxy laminates, giving ∼1.5 kJ/m^2 toughness enhancement—a value several times that of typical aerospace-grade laminates.[14]

One fiber architecture of particular interest is carbon fiber circumferentially coated with radially aligned arrays of carbon nanotubes (CNTs), which could in principle be used to prepare composites with superior in-plane properties while simultaneously providing interlaminar and intralaminar reinforcement and multifunctional benefits such as electrical and thermal conductivity enhancement. Achieving this type of growth morphology on carbon fibers would therefore be highly desirable for industrial applications and could even serve to replace the sizings used today to provide an interphase region to improve adhesion of carbon fibers to matrix resins (among other functions). In fact, carbon-nanofiber-coated carbon fibers have been prepared by numerous groups through various approaches, with reports dating back as far as 1991[21] (noting that growth of SiC whiskers on carbon fibers has been a related approach of interest since the 1960s[22−26]). Downs and Baker published several works showing carbon nanofibers grown on carbon fibers by catalytic CVD from ethylene employing Ni/Cu catalysts[21,27] and demonstrated that doing so results in an improvement in apparent shear strength between fiber and polyvinylethylacetate matrices.[27] More recently, Kepple et al. showed that laminates prepared with carbon fiber weaves coated with unaligned CNTs can also result in improvements in fracture toughness of 0.2−0.3 kJ/m^2 and an improvement of ∼10% in flexural modulus in three-point bending over control laminates.[28]

Despite these promising results, however, growth of CNTs on high-performance fibers has been shown to result in substantial loss of the underlying fiber's tensile strength and stiffness.[29] Qian et al. assessed the apparent fiber-matrix adhesion shear strength of CVD-grown unaligned-CNT-coated carbon fibers in an epoxy matrix at the single-fiber level and showed an improvement of ∼57% in this value in fiber pull-out tests[29] but demonstrated that preparation of such fibers also results in a 55% reduction in fiber tensile strength (from 3.5 to 1.6 GPa). Works by Sager et al. and Mathur et al. employing floating catalyst CVD processes also show similar levels of degradation in tensile strength as well as tensile modulus of high-performance carbon fibers following CNT growth.[30,31] One work reported that CNTs have been grown on high-performance carbon fibers (Cytek T650 and IM-7) without substantial reduction in fiber tensile properties based on statistical arguments, however the work relies on unusually wide error bars in single-fiber tensile strength measurements in which the reported mean tensile strength and stiffness of the resulting fibers are substantially lower than those of the starting materials.[32] Numerous additional works[28,29,32−41] describing various methods for growing CNTs on carbon fibers[28,29,32−35,39−41] or attaching prefabricated CNTs to carbon fibers[36−38] also exist; however, they neglect to characterize effects on fiber tensile properties, and in many cases, utilize low-grade carbon fibers (<3 GPa baseline tensile strengths) and/or involve harsh chemical treatments which damage the carbon fibers, thereby making them of limited utility for aerospace composites applications.

Herein lies the fundamental problem in preparing hierarchical nanoengineered carbon fibers—growth of CNTs on high-performance carbon fibers by CVD has, to date, resulted in substantial reduction in fiber tensile strength and stiffness, and apparently the CNT growth process somehow damages carbon fiber and only introduces microstructural benefits at the expense of in-plane properties. Notably, this trade-off appears to be specific to carbon fiber—such a compromise is not the case for analogous alumina/epoxy FFRP systems.[17]

In this paper, we demonstrate two new approaches for growing aligned and unaligned arrays of CNTs on high-tenacity aerospace-grade ex-PAN carbon fibers that, for the first time, enable growth of CNTs on carbon fiber surfaces while simultaneously preserving carbon fiber strength and stiffness. In the first approach, catalyst-loaded fibers are CVD processed using ethylene and hydrogen while being tensioned to ≥12% of their tensile strength, resulting in aligned CNT growth while simultaneously preserving fiber strength and stiffness despite exposure to temperatures in excess of 700 °C. Fiber-damaging etching processes typically used to facilitate adhesion of CNT catalyst precursors to the carbon fiber are replaced with solution-based noncovalent polyelectrolyte coatings employing the free acid or potassium salt of poly(styrene-*alt*-[maleic acid]) and an optional sol−gel-derived alumina coating used to promote CNT alignment. In the second approach, CNT growth via CVD employing carbon dioxide and acetylene at 480 °C[41]—below the observed critical strength-loss temperature—is achieved and shown to have no deleterious effects on fiber strength or stiffness. These approaches exploit previously unidentified mechanisms underlying production of hierarchical carbon fibers and demonstrate two scalable, facile methods for doing so that are compatible with current carbon fiber manufacturing technologies.

2. EXPERIMENTAL SECTION

Materials. Unsized (i.e., never-sized), never-surface-treated carbon fiber tow (TohoTenax product number HTR40 N00 24k 1550tex) was used as substrates for most experiments. (Note: This product was obtained through industrial liaisons and is not available commercially. The equivalent commercial version, HTA40 F22 24k 1550tex, is surface-

treated and sized.) Unsized AS4 fibers were also used as substrates in some experiments. Unsized fiber was chosen in order to eliminate possible fiber damage caused by desizing procedures such as thermally decomposing the sizing under inert atmosphere or high-temperature interaction between the fiber and any unremoved sizing.

Aluminum tri-*sec*-butoxide (ATSB, Sigma-Aldrich product number 201073, 97%), 2-methoxyethanol (MeOEtOH, Sigma-Aldrich product number 185469, ≥99.0%), acetylacetone (acac, Sigma-Aldrich product number 10916, ≥99.5%), potassium carbonate (Sigma-Aldrich product number 209619, ≥99.0%), nitric acid (Sigma-Aldrich product number 438073, ACS grade), poly(styrene-*alt*-[maleic anhydride]) (PSMA, Sigma-Aldrich product number 477699, 99%, M_w = 350 000), sodium hydroxide (Mallinckrodt product number 7708−06, ACS grade), and analytical reagent grade deionized water (Ricca Chemical Company product number 9150−1) were used as received.

Aqueous solutions with varying concentrations of poly(styrene-*alt*-[maleic acid]) (h-PSMA, the hydrolyzed form of PSMA) were prepared according to the method of Stroock et al.[42] Solutions were prepared by dissolving 1.4, 4.2, or 7.0 g of PSMA (corresponding to concentrations of 0.5, 1.5, and 2.5 wt %, respectively) in 25 mL of acetone with gentle heating. The PSMA solution was then added to 300 mL of 0.3 M NaOH in deionized water with stirring and allowed to react for 3 h, after which it was acidified with 0.1 M HNO_3 to a pH of 8. The acetone in the solution was then removed with a rotary evaporator.

Ar, He, H_2, C_2H_4, and acetone-free 10% C_2H_2 in Ar blend (Airgas, ultrahigh-purity grade, >99.999%) were used for thermochemical processing and CVD as received.

Noncovalent Functionalization of Carbon Fibers with h-PSMA. h-PSMA was coated over the fibers by dip-coating a tow in aqueous h-PSMA solution for ∼5 min and subsequently allowing the tow to dry in air (which took ∼120 min) or blow-drying with cool air (which took ∼9 min). Upon removal of the tow from h-PSMA solution the tow became noticeably stiff and difficult to peel apart. To improve coating of fibers in the inner tow, the tow could be dabbed up and down in the h-PSMA solution (as is done to clean a watercolor paintbrush) over the 5-min period.

Application of Alumina Barrier Coating to Carbon Fibers. h-PSMA-coated fibers were sheathed with a sol−gel-derived alumina coating upon which a catalyst for CNT growth was added. Two sol−gel processes for depositing alumina were investigated—an alkoxide-based approach and an epoxide-assisted approach.[43] In the alkoxide-based approach, a solution of 50 mL of MeOEtOH, 1.25 mL of ATSB, and 0.5 mL of acac was prepared. Next, carbon fiber substrates were rinsed with acetone followed by 2-propanol and baked dry on a hot plate at 80 °C. The carbon fibers were then soaked in the alkoxide solution and baked in air at 200 °C. The process was repeated 3−6 times to build up a thicker (up to ∼1 μm) alumina coating. In the epoxide-assisted approach, 2.96 g $AlCl_3{\cdot}6H_2O$ was dissolved in a mixture of 20.0 g (20.0 mL) deionized water and 20.0 g (25.4 mL) 2-propanol. The mixture was stirred until the salt had fully dissolved. Next, 7.86 g (9.5 mL) propylene oxide was added slowly into the solution via syringe through an 18-gage stainless steel needle with stirring. The solution was then stirred another 5 min and allowed to solify. Gel time was ∼4 h. Alternatively, a solution of 10.0 g (10.0 mL) deionized water and 7.89 g (10.0 mL) absolute ethanol could be used as the solvent system instead of a mixture of deionized water and 2-propanol. In this case the gel time was reduced to ∼1 h 40 min. Gel time could be further adjusted for either of these processes by increasing the amount of solvent used; however, this also results in an increase in porosity.

CVD Growth of CNTs on Alumina-Coated Carbon Fibers. Catalyst precursor was applied to h-PSMA/alumina-coated fibers. First, a catalyst solution of 0.050 M $Fe(NO_3)_3{\cdot}9H_2O$ in 2-propanol (IPA) was prepared and aged with stirring for 0−2 h. Solution aging time was examined as a parameter for controlling CNT diameter and density as iron oxide nanoparticles continually grow in the solution during this time frame and eventually precipitate. h-PSMA/alumina-coated fibers were subsequently dip-coated into this solution for ∼5−30 min.

h-PSMA/alumina/Fe^{3+}-coated fibers were CVD-processed for CNT growth. CVD growth of CNTs was performed in a fused quartz tube (54-mm outer diameter, 50-mm inner diameter, 137-cm length) heated by a three-zone split-hinge tube furnace (Lindberg/Blue M model HT55667C, 30-cm heated zone lengths). (Note: Calibration via in situ thermocouple measurement is strongly advised for repeatable results.) In a typical process, specimens were placed in the fused quartz process tube at the center of the third zone. The tube was then flushed with a flow of 2070 sccm He for 10 min to displace oxygen from the tube. Next, a flow of 1040 sccm H_2 gas was introduced and He was turned off. The sample was then heated to 650 °C under H_2 gas over the course of ∼8 min to reduce iron oxide nanoparticles on the specimen to catalytically active iron. The sample remained at these conditions for an additional 7 min to further reduce remaining iron oxide nanoparticles. A flow of 316 sccm ethylene was then added for 5 min to facilitate CNT growth. Lastly, the flow of He was increased to 2070 sccm, the H_2 and C_2H_4 were turned off, and the sample was allowed to cool to room temperature under He flow.

Preparation of K-PSMA Ion Exchange Polyelectrolyte. Various formulations for preparing K-PSMA were explored. In the method most optimal for CNT growth, a solution of 1.5 wt % h-PSMA is prepared as described above. The h-PSMA polyacid is then neutralized by stirring solid K_2CO_3 into the solution. At first, the K_2CO_3 simply dissolves in the solution, but upon further addition, evolution of a CO_2 fizz results. K_2CO_3 is added until CO_2 fizz no longer results upon further addition. This point corresponds to a solution pH of ∼11 or ∼0.79 g K_2CO_3/10.00 g 1.5 wt % h-PSMA solution.

Noncovalent Functionalization of Carbon Fibers with K-PSMA. Carbon fiber tows (∼10 cm long) were cut and taped at one end with masking tape (3M 2600) for ease of handling. K-PSMA was coated over the fibers by dip-coating a tow in aqueous K-PSMA solution for ∼5 min and subsequently allowing the tow to dry in air (which took ∼120 min) or blow-drying with cool air (which took ∼9 min). Upon removal of the tow from K-PSMA solution, the tow became noticeably stiff and difficult to peel apart, but less so than when coating with h-PSMA. To improve coating of fibers in the inner tow, the tow could be dabbed up and down in the h-PSMA solution (as is done to clean a watercolor paintbrush) over the 5-min period.

K-PSMA-coated fibers were then dip-coated with iron catalyst precursor solutions. In a typical process, 0.050 M $Fe(NO_3)_3{\cdot}9H_2O$ in 2-propanol (Fe^{3+}/IPA) was used. Solutions were aged for 30 min, 60 min, and 90 min prior to dip-coating, with 60 min being the optimal time. K-PSMA-coated fibers were optionally dip-coated before the K-PSMA deposit was dry, others were dip-coated after it was dry. Alternatively, 0.1 M aqueous $Fe(NO_3)_3$ was used to dip-coat catalyst precursor. After dip-coating with catalyst, the masking tape at the end of the tow was cut off. At this point, the tow was sufficiently stiff from and held together by the K-PSMA coating that handling of the fibers was possible without tape.

CVD Growth of CNTs with K-PSMA-Coated Carbon Fibers. Fe^{3+}/K-PSMA-coated fibers were CVD processed for CNT growth using the oxidative dehydrogenation process described by Magrez et al.[41] We found that the temperatures reported by Magrez et al. underestimate the optimal growth temperature for similar substrates in our system by ∼80 °C. As such, the optimal growth temperature for carbon-supported iron reported by Magrez et al. (400 °C) was converted to a set point of 480 °C for our system. Samples were placed in a dedicated fused quartz process tube (25 mm outer diameter × 22 mm inner diameter × 30 cm length) and heated in an electric clam-shell tube furnace (Lindberg/Blue M MiniMite). Samples were positioned at 75% along the length of the heated zone. First, a flow of 750 sccm Ar was introduced into the reactor for 2 min to displace oxygen from the process tube. Next, a flow of 400 sccm H_2 was added and the Ar flow was lowered to 200 sccm Ar. The samples were then heated to a set point temperature of 480 °C under H_2/Ar flow to reduce and coarsen iron ions bound to the coated fiber surfaces to iron nanoparticles. Once at this temperature, a flow 17 sccm CO_2 and 167 sccm 10% C_2H_2 in Ar (acetone-free) were introduced and the H_2 and Ar deactivated. The samples were soaked under these conditions for 15 min after which a flow of 750 sccm Ar was introduced and the CO_2 and C_2H_2/Ar mixture were deactivated. The furnace was then opened and the samples were allowed to cool to ambient conditions. Between CNT growths, the quartz process tube was baked in air at 750 °C for ∼20 min to remove deposited organic matter. In one variation of this process, samples were

not treated with H_2 on ramp-up to the set point temperature to evaluate the necessity of reducing the Fe^{3+} prior to growth; however, best results were obtained with H_2 flow.

Efficacy of various K-PSMA formulations and catalyst application methods for facilitating CNT growth was assessed by the presence, areal density, and length of CNTs on tows following CVD processing as observed by SEM.

Preparation and Mounting of Carbon Fiber. Unsized fibers were rinsed with acetone and evaporatively dried in air. Single fibers were carefully extracted from the 24k tow using Q-Tips, which gently latch onto the fibers and pull them out from the other fibers. Care was taken not to stretch fibers when pulling them out to avoid pretensioning of the fiber. (Note that the force required to break a single carbon fiber is ∼40−180 mN, or ∼0.01−0.04 lbf, corresponding to a stretch of only ∼150−300 μm.) The single fibers were then mounted into a rectangular two-piece milled graphite frame to hold them in place for handling and processing (see the Supporting Information). Fibers were mounted into the frame by stringing lengthwise across the bottom half of the frame with slack on either side and then setting the top half of the frame on top. This held the fibers in place by compression. Up to five fibers could be mounted at a time. If coatings were to be applied to the fibers, masking tape was used to hold the frame together until the fibers were ready for heat treatment at which point the masking tape was peeled off and any adhesive residue was gently scrubbed from the frame with acetone.

Application of Coatings and CVD Growth of CNTs on Single Carbon Fibers. Graphite frames loaded with isolated single carbon fibers were placed into a "boat" of Parafilm (i.e., the frame was wrapped with Parafilm on all sides except the top) to allow for filling of the frame with liquid. Using a Pasteur pipet, 2.5 wt % aqueous h-PSMA solution was injected into the frame until the fibers were submersed (note that the frame is wetted in this process). The fibers were allowed to soak in the solution for 2 h, after which the solution was drained using a Pasteur pipet and the fibers were allowed to evaporatively dry in air overnight.

Graphite frames loaded with isolated single fibers were placed into a new Parafilm boat as described above. Using a Pasteur pipet, a solution containing 2.5 vol % ATSB in MeOEtOH was injected into the frame until the fibers were submersed as described above. The fibers were allowed to soak for 5 min after which they were heated at 200 °C in a convection oven and cooled in air for 3 min. This process was repeated three times. The coated fibers were then allowed to dry 30 min at room temperature prior to further processing.

A solution of 0.050 M $Fe(NO_3)_3{\cdot}9H_2O$ in 2-propanol was prepared and stirred for 1−2 h. Graphite frames loaded with isolated single fibers were placed into a new Parafilm boat as described above. Using a Pasteur pipet, the frames were then filled with the iron nitrate solution aged no more than 2 h until the fibers were submersed. Shortly after (∼5 min), the frame was drained, the fibers were allowed to dry overnight, and the Parafilm boat was removed.

Atmospheric thermal CVD growth of CNTs was performed as described above for alumina-coated carbon fibers.

Thermochemical Processing of Single Fibers Under Tension. The role of tension during thermochemical processing of carbon fibers was evaluated using a special all-graphite single-fiber tensioning frame in which fibers were tensioned in situ with a set of special graphite clamp-on weights used to impart up to 0.5 GPa of tension ($\bar{\Xi}$ = 0.12) into single carbon fibers (see the Supporting Information). A set of tungsten-core, graphite-shell weights was also produced and enabled application of tension up to 3.2 GPa (for conditions of $\bar{\Xi}$ = 0.45 and greater). Fibers were mounted, coated, and CVD-processed, similar to with the nontensioning frame. Engineering diagrams and detailed experimental procedures with illustrations for mounting, coating, tensioning, and CVD processing single carbon fibers using this tensioning system are provided in the Supporting Information.

Single-Fiber Tensile Testing. Single-fiber tensile tests were performed in a universal testing machine (Nano-UTM, MTS Nano Instruments) according to the ASTM D3379−75 standard.[44] This standard was selected over the ISO 1156 standard,[45] another candidate single-fiber tensile test standard, because ASTM D3379−75 factors in strain rate, which we have observed can significantly impact the measured tensile strength values for single carbon fibers. A baseline data set for as-received fibers was established each day that tensile tests were run to normalize variations arising from machine alignment and variations in materials properties along the tow spool. As an extra validation step, conclusions regarding a sample type are drawn based on differentials run against their respective baseline data set. Detailed testing procedures used for the single-fiber tensile tests are provided in the Supporting Information. Stress−strain plots for all single fiber tests performed in this work are available elsewhere.[46]

Compositional Characterization. Thermogravimetric analysis (TGA) of carbon fibers was performed using a TA Instruments Discovery TGA with 100-μL platinum HT sample pan (TA Instruments part number 957571.901). For mass retention measurements as a function of temperature, samples were equilibrated at 25 °C, soaked isothermally for 25 min, ramped at 10 °C/min to 900 °C, and then soaked isothermally for 5 min. For mass retention measurements as a function of time at a given temperature, samples were equilibrated at 25 °C, soaked isothermally for 30 min, ramped at 100 °C/min to the target set point (400, 500, or 650 °C), and soaked isothermally for 60 min. X-ray diffraction (XRD) of carbon fibers was performed with a PANalytical X'Pert Pro MPD with RTMS detector using Cu Kα radiation, a voltage of 45 kV, and a current of 40 mA with parallel-beam optics. Samples were optionally heated to 400, 500, or 650 °C in situ with an Anton Paar HTK-1200N oven under He atmosphere during analysis. Elemental composition was determined using Auger spectroscopy with a Physical Electronics (PHI) Model 700 Scanning Auger Nanoprobe. Field-emission scanning electron microscopy (FE-SEM) was also performed with this system. Carbon fiber tows were mounted to the sample holder with adhesive carbon tape and then spread, firmly pressed into place, and trimmed. Analysis windows were 5 × 20 μm along the length of a fiber and positioned on the fiber center to avoid angle-dependent signal shifts. Measurements were made on fibers separated from other fibers by a distance of at least 5 μm to avoid scattering of secondary Auger electrons from adjacent fibers. A charge neutralizer was not used. Scanning electron microscopy (SEM) was performed with JEOL JSM-6060 operating at 5 kV-15 kV (depending on sample composition) with a spot size of 40−50 at a working distance of 10 mm. Transmission electron microscopy (TEM) was performed with a JEOL 2010 with an acceleration voltage of 200 kV.

3. RESULTS AND DISCUSSION

3.1. Coatings for Enabling CNT Growth on Carbon Fibers. To facilitate CNT growth by CVD, catalyst nanoparticles must be present on the carbon fiber surface. For composites applications, aligned CNTs are of greatest interest as they facilitate capillarity-driven wetting by matrix materials and enable the CNTs to reinforce the matrix material in a cooperative fashion.[15,16,19] Carbon fibers are challenging substrates upon which to grow CNTs for a number of reasons, however. First, the majority of the tensile load carried by a carbon fiber is transmitted in the outer skins of the fiber; as such, any disruption to the surface can result in a mass-disproportionate loss of tensile properties.[47] Second, the outer surface of the fiber is highly graphitic and therefore exhibits low wettability, providing few active binding sites to which coatings can be applied. Third, commonly employed CNT catalysts (e.g., metals such as Fe, Ni, etc.) react with or dissolve carbon at CNT growth temperatures (700−900 °C)—a property that has been speculated to be related to their efficacy in CNT growth.[48,49] Fourth, carbon reacts with oxygen, water, and hydrogen at temperatures above 400 °C. In addition, many substances common in the environment catalyze microstructural transformations in carbon at these temperatures (e.g., Na^+ and K^+ ions from skin).

Thus, it is challenging to adhere CNT catalyst materials to carbon fiber without an additional chemical step that would also result in reduction of fiber tensile properties. Avoiding surface modification alone is not enough to prevent reduction in tensile

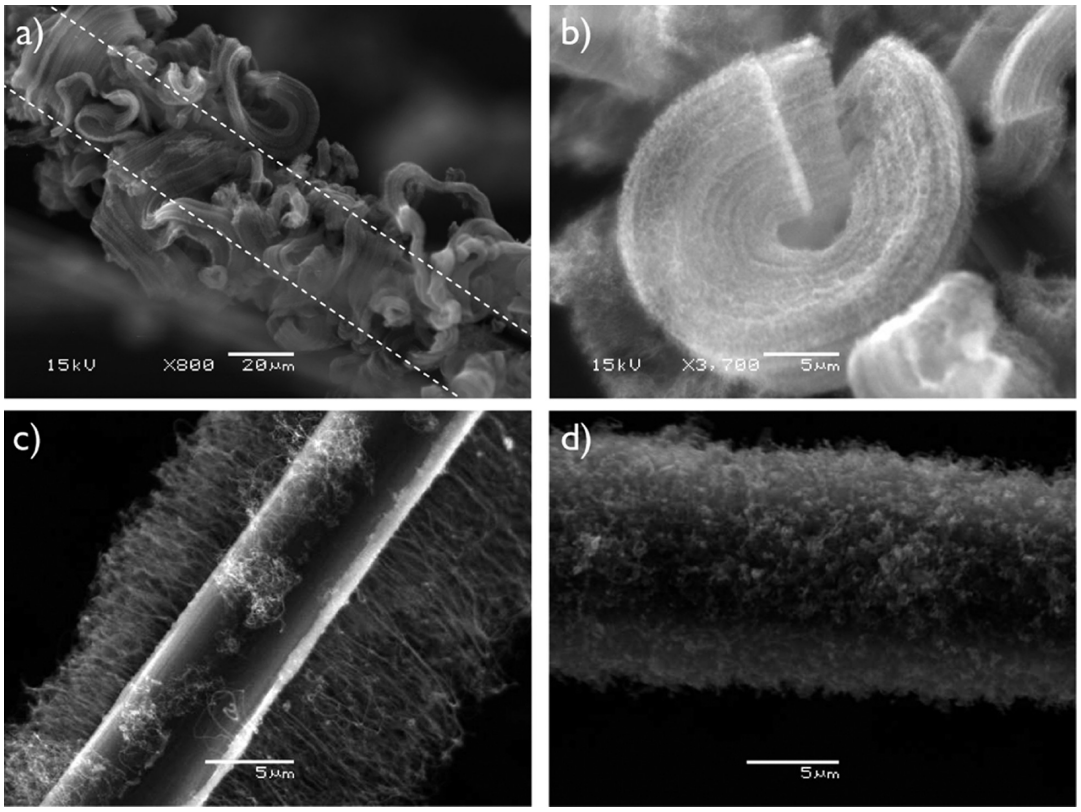

Figure 1. CNT-coated carbon fibers produced in this work: (a) HTR40 carbon fiber covered with highly aligned bundles of multiwall carbon nanotubes grown from Fe catalyst nanoparticles on sol−gel-derived alumina barrier coating (fiber location noted with white dashed lines); (b) detail of aligned CNT bundle extending off of carbon fiber surface; (c) cross-sectional view of aligned CNTs grown on a single carbon fiber as isolated fiber (sparse CNT density is an artifact of single-fiber processing); (d) carbon fiber coated with unaligned CNTs.

properties: even in cases where catalyst material is applied without surface etching such as in in situ deposition of floating catalyst particles during CNT growth,[31,32,35] damage to the fiber at the CNT growth temperatures still occurs. Accordingly, we sought to eliminate direct chemical modification of the carbon fiber surface to minimize damaging the tensile-stress-transmitting microstructure of the fiber's outer skins and instead focused on approaches that do not involve acid, base, or electrochemical etching of fibers (not including acidic or alkaline processing steps that are nonetching in nature). Additionally, processes such as e-beam evaporation that are nonconformal and difficult to scale in this context were also avoided.

In our experience, and consistent with other reports in the literature, growth of CNTs from catalyst nanoparticles on carbon fiber surfaces generally results in substantially unaligned ("scraggly") CNT morphologies.[46] This is in contrast to alumina substrates (such as alumina fibers), where aligned CNT growth is routinely achieved provided a sufficiently high density of catalyst nanoparticles. As such, we found that disguising carbon fiber with an alumina barrier coating enables excellent aligned CNT growth by CVD.[46,50] A survey of various alumina deposition methods revealed that facile solution-based sol−gel processing can be used.[46,50] To address the problems of poor wettability and shrinkage/cracking associated with mass-loss in drying of sol−gel-derived oxide films, we developed a method of noncovalently functionalizing carbon fibers with amphiphilic polymers derived from poly(styrene-*alt*-[maleic anhydride]) (PSMA).[42,46,50,51] In this approach, fibers are dip-coated with aqueous solutions of the hydrolyzed form of PSMA, poly(styrene-*alt*-[maleic acid]) (h-PSMA), which adsorbs to the fiber via hydrophobic $\pi-\pi$ interactions to present a polar carboxylic acid surface over the fiber without any covalent modification of the fiber microstructure. This approach was found to both facilitate adhesion and eliminate cracking of alkoxide-derived alumina films and alumina films synthesized through epoxide-assisted gelation applied via dip coating.

We also sought to load catalyst nanoparticle precursors (specifically iron oxide nanoparticles) onto carbon fibers without alumina barrier coating. In this approach, carbon fibers were first dip-coated with 1.5 wt % aqueous h-PSMA and then dried and subsequently dip-coated into solutions of 0.050 M Fe-$(NO_3)_3{\cdot}9H_2O$ in 2-propanol aged 1−2 h. The Fe^{3+}-based precursor did not to adhere to h-PSMA-coated fibers and so to facilitate adhesion of Fe^{3+} ions and iron oxide nanoparticles, an ion-exchange polyelectrolyte, the potassium salt of h-PSMA (K-PSMA), was developed. In contrast to h-PSMA-coated fibers, Fe^{3+}-based solutions loaded iron efficiently and uniformly onto K-PSMA-coated fibers producing catalyst-loaded fibers suitable for high-yield CNT growth. As such, K-PSMA was employed as a noncovalent coating for loading catalyst directly onto carbon fibers for select experiments in this work. Details about the optimization of K-PSMA for barrier-free CNT growth on carbon fibers are available elsewhere.[46]

3.2. Characterizing the Mechanochemical Response of Carbon Fibers to Thermal Processing. To understand the origins of strength loss upon CVD processing of carbon fibers, we characterized the mechanochemical response of two different never-sized aerospace-grade carbon fibers (HTR40 and AS4) to CVD gases used for CNT growth, the presence of our noncovalent and sol−gel-derived functional coatings used to

enable CNT growth, and tensioning of the fibers at CNT growth temperatures. Although processing carbon fiber in tow or weave form is useful for composites applications, uneven loading of coatings arising from bundling of fibers and from capillary effects makes analysis of fibers processed in these forms precarious. To unambiguously characterize the influence of the presence of a coating on fiber properties, the fiber should be coated, thermally processed, and directly tested in isolation from other fibers. To best evaluate the mechanochemical response of carbon fibers to the aforementioned process variables of interest, we developed a methodology for manipulating, coating, tensioning, and thermally processing individual 7-μm-diameter carbon fibers (see Experimental Section and Supporting Information for more details). The effects of CVD processing on uncoated and coated carbon fibers was investigated with single-fiber tensile tests according to the D3379−75 standard.[44] Carbon fiber strength is inherently limited by flaws in the fibers and is characterized here using a Weibull distribution.[52] The Weibull distribution represents the probability of failure for a fiber at a particular tensile load (i.e., its tensile strength). The probability of failure is given by

$$p(x) = \begin{cases} \frac{\alpha}{\beta}\left(\frac{x}{\beta}\right)^{\alpha-1} e^{-\left(\frac{x}{\beta}\right)^{\alpha}} & x \geq 0 \\ 0 & x < 0 \end{cases} \quad (1)$$

where x is the parameter of interest (here tensile strength), β is the location parameter, and α is a scale factor (or "Weibull modulus"). It is assumed that fibers have random flaws distributed along them which result in fiber failure according to a weakest-link-in-chain model, and that these flaws follow Weibull−Poisson statistics. Accordingly, the location parameter can be approximated by the mean tensile strength

$$\beta \approx \bar{x} = \bar{\sigma} \quad (2)$$

and the Weibull modulus, α, can be approximated as the ratio of the mean tensile strength to standard deviation in tensile strength, $S(\bar{\sigma})$

$$\alpha \approx \frac{\bar{x}}{S} = \frac{\bar{\sigma}}{S(\bar{\sigma})} \quad (3)$$

These approximations are employed in the data reported here. According to the ASTM standard, a minimum of 15 successful tests is required for calculation of a Weibull distribution to be considered valid;[44] as such, each condition surveyed involved preparation and testing of at least 15 samples with the exception of a few preliminary diagnostic tests (see the Supporting Information). We note that the Weibull distributions presented here may be wider than the true distribution of fiber properties in a tow as they include all measurements regardless of fiber break location.

Single carbon fibers were coated with h-PSMA and with full Fe^{3+}/alumina/h-PSMA coating and CVD processed. CNT growth on single carbon fibers was achieved with the latter coating (Figure 1). Tabular data for the mean tensile strength, tensile stiffness, and Weibull parameters for coated and uncoated fibers surveyed are provided in the Supporting Information. A comparison of the tensile strength distributions of as-received HTR40 fibers, CVD-processed (i.e., subjected to the gases and heating cycles used for CNT growth, which may or may not have resulted in CNT growth) h-PSMA-coated HTR40 fibers, and CVD-processed Fe^{3+}/alumina/h-PSMA-coated HTR40 fibers is shown in Figure 2a. Consistent with previous reports, a substantial reduction in tensile strength (~45−55%) over the as-received fibers for both coated sample types is observed. Notably, this is comparable to strength losses attributable to acid etching and subsequent CVD processing with Fe nanoparticles

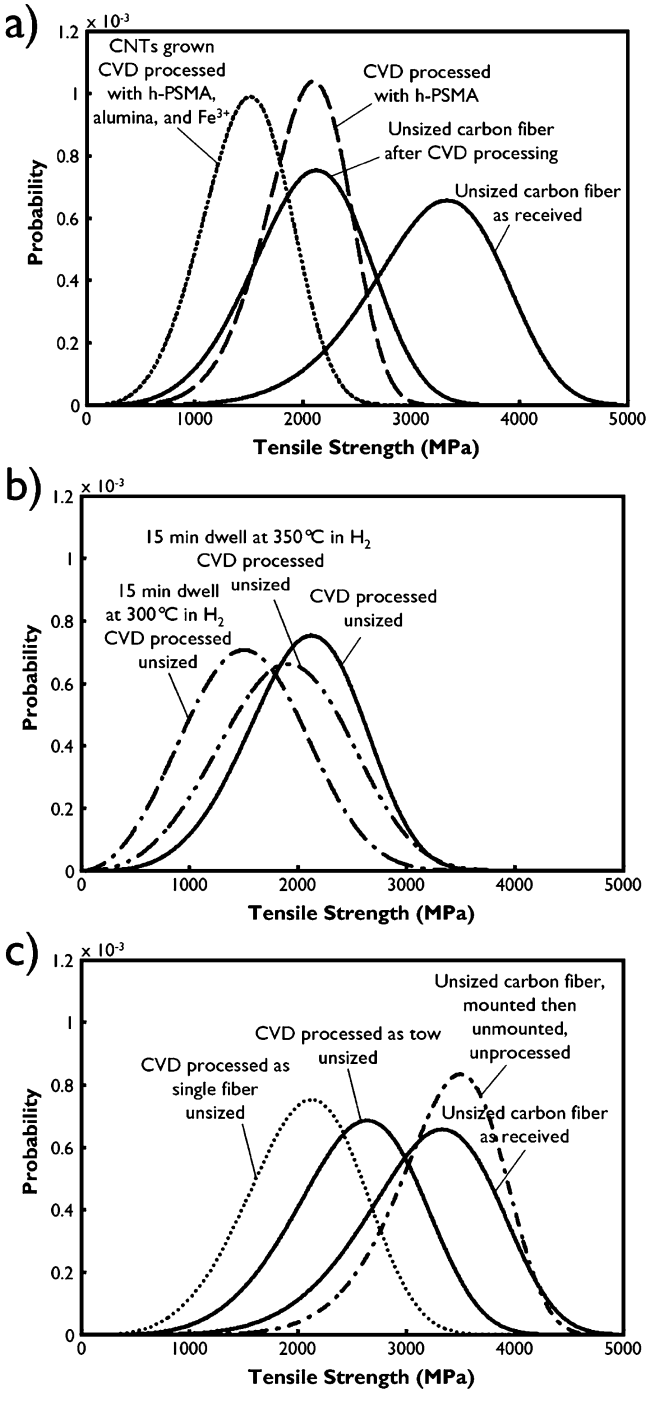

Figure 2. Weibull distributions calculated from single-fiber tensile tests showing the effects of various processing conditions on the tensile strength of HTR40 carbon fibers: (a) effects of exposure to CNT growth gases and heating cycles ("CVD processing") on unmodified fibers, h-PSMA-coated fibers, and full h-PSMA/alumina/Fe^{3+}-coated fibers compared with as-received fibers; (b) effects of hydrogen prior to CNT growth process; (c) effects of thermally processing fibers in isolation versus in tows and mounting single fibers into processing frame.

dx.doi.org/10.1021/am4006385 | ACS Appl. Mater. Interfaces 2013, 5, 4892−4903

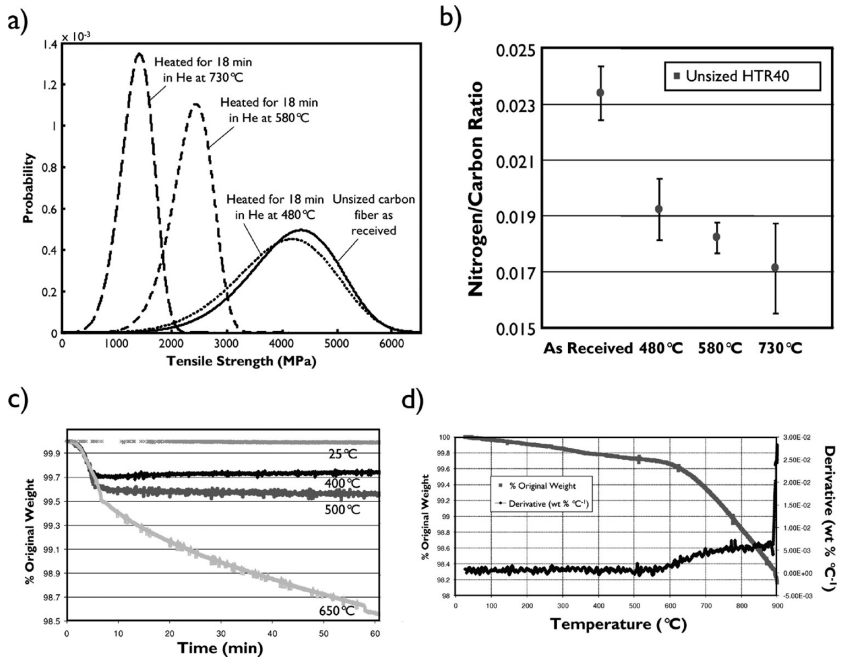

Figure 3. (a) Effects of heat treatments in He on tensile strength of HTR40 carbon fibers as a function of temperature, showing strength loss arising from heat treatment at 580 and 730 °C but not 480 °C; (b) elemental nitrogen-to-carbon ratio of the surface of unmodified HTR40 carbon fibers heat-treated in He as a function of heat treatment temperature; (c) thermogravimetric analysis (TGA) of HTR40 carbon fibers in He atmosphere showing mass retention at 25, 400, 500, and 650 °C as a function of time; (d) TGA of HTR40 carbon fibers in He showing mass retention as a function of temperature, revealing a temperature-activated process beginning around 550 °C.

present directly on the carbon fiber surface.[27,29] Further investigation, however, revealed that the majority of this strength loss was not due to the presence of the functional coatings used: remarkably, uncoated fibers exposed to the CVD environment (i.e., CVD-processed but without catalyst) also exhibited a substantial (~36.8%) loss in tensile strength compared to never-processed fibers (Figure 2a). An additional (~28.2%) loss in tensile strength past this value is observed for the CNT-growing Fe^{3+}/alumina/h-PSMA-coated fibers compared to CVD-processed uncoated fibers (Figure 2a). As a result, it was hypothesized that something in the CVD atmosphere may be corrosive to the carbon fibers, and that additional incremental strength loss was being incurred from an aspect related to the full Fe^{3+}/alumina/h-PSMA coating (e.g., insufficient coating coverage resulting in contact between carbon fiber and iron, diffusion of iron through the barrier coating, damage due to reaction between the h-PSMA coating and carbon fiber, etc.) Notably, CVD processing of fibers coated only with h-PSMA (~34% strength loss) was found to result in a similar strength loss to CVD processing the fibers uncoated (~30% strength loss), thus eliminating it is a direct cause for the additional strength loss associated with use of the full coating and validating the use of h-PSMA as a carbon-fiber-compatible functionalization strategy.

One potential fiber-damaging agent in the CVD atmosphere considered was residual oxygen remaining in the process tube upon ramp-up to the temperature set point (despite flushing of the tube with He prior to heating).[53] To test this, processes employing a 15-min H_2 dwell at a low temperature (300 or 350 °C) prior to reaching the process set point, designed to quench any residual oxygen, were examined. The results of these experiments are summarized as Weibull distributions Figure 2b (see also the Supporting Information). No substantial improvement in tensile strength loss was observed using this approach; in fact, a slight degradation is observed.

Another possible source of strength loss considered was the possibility of stresses introduced during mounting and unmounting of the single fibers resulting in the formation of flaws prior to or during CVD processing (Figure 2c). The mounting process was not found to induce a statistically significant change in tensile strength. Processing as single fibers as opposed to in tows was found to introduce an incremental additional amount of strength loss, which we attribute may be due to the absence of collective off-gassing present in tows: following from Le Châtlier's principle, fibers heated in the presence of a higher concentration of off-gassed products arising from fiber decomposition (e.g., HCN) would tend toward an equilibrium state of less decomposition, thereby resulting in a higher rate of fiber decomposition and thus strength loss for bare fibers. However, as the strength loss attributable to processing as single fibers is relatively minor and is an artifact specific to this experimental procedure, it was discounted as the major source of properties degradation observed by us and others.

The surprising loss of tensile strength and stiffness caused by CVD processing of both coated and uncoated single carbon fibers revealed that the primary source of properties degradation in CNT growth on carbon fibers must lie in some aspect of the CVD process itself and not in interactions between the fiber and coatings or catalysts used to facilitate CNT growth. This intriguing observation led to a series of experiments to characterize the response of carbon fibers to simply heating in inert atmospheres. In one set of experiments, unsized, uncoated HTR40 fibers were heated to 480 °C, 580 °C, and 730 °C such that the time the fibers were at or above 480 °C was equal to 18 min. Figure 3a displays Weibull distributions calculated from tensile tests from samples processed under these conditions. No loss in tensile strength is observed for fibers thermally processed in He at 480 °C; however, substantial strength loss is observed in samples heated to 580 °C, and even further strength loss is

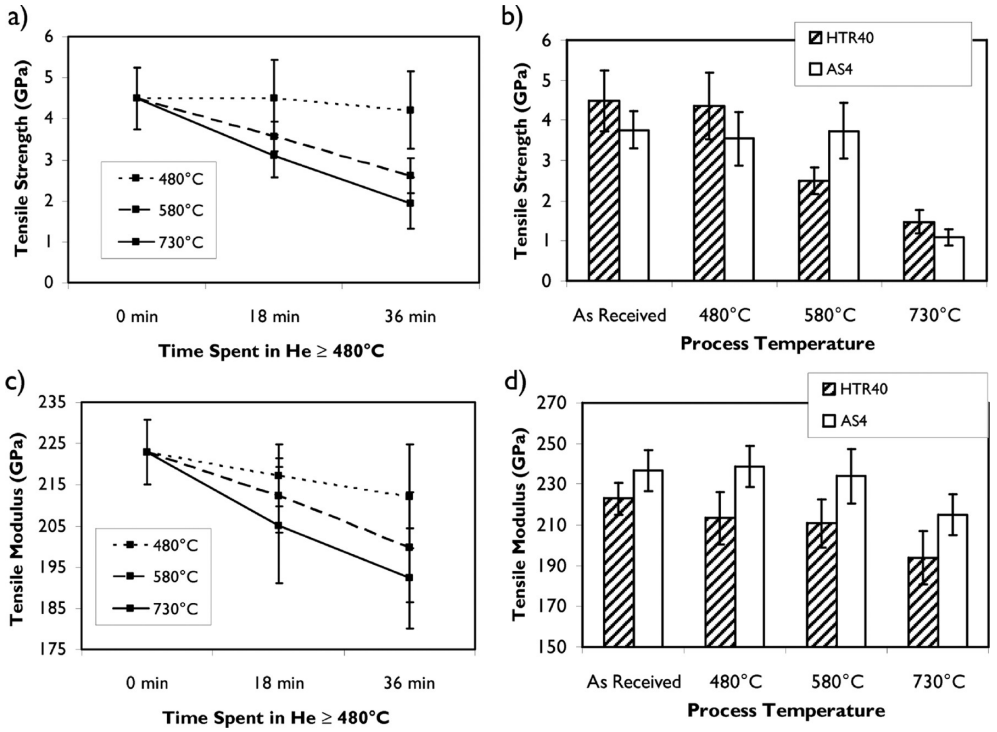

Figure 4. (a) Tensile strength of HTR40 fibers as a function of duration and temperature of heat treatment in He; (b) comparison of the effects of heat treatment in He on the tensile strength HTR40 and AS4 fibers; (c) tensile modulus of HTR40 fibers as a function of duration and temperature of heat treatment in He; (d) comparison of the effects of heat treatment in He on the tensile modulus of HTR40 and AS4 fibers.

observed in samples heated to 730 °C. Extending the length of the heat treatment has a further detrimental effect at 580 and 730 °C, but not noticeably at 480 °C, that is, the degree of damage is not a function of temperature alone. Both strength (Figure 4a and b) and stiffness (Figure 4c and d) are further compromised with longer treatment time at these temperatures. Thus it appears that a thermally activated process is responsible for the observed degradation in tensile properties and occurs above 480 °C.

For practical utility, equations for predicting the tensile strength and tensile modulus of HTR40 carbon fibers following heat treatment in inert atmosphere were fit to the data presented in panels a and c in Figure 4 using linear regressions along the dimensions of temperature and time

$$\begin{aligned}\bar{\sigma}\ (T, t \geq 480°\mathrm{C}) &= ([-0.000241\ \mathrm{GPa}\ °\mathrm{C}^{-1}\ \mathrm{min}^{-1}]Tt \\ &\quad + [0.100\ \mathrm{GPa}\ \mathrm{min}^{-1}])t \\ &\quad + ([-0.000357\ \mathrm{GPa}\ °\mathrm{C}^{-1}]T + [4.71\ \mathrm{GPa}])\end{aligned} \tag{4}$$

and

$$\begin{aligned}\bar{E}\ (T, t \geq 480°\mathrm{C}) &= ([-0.00241\ \mathrm{GPa}\ °\mathrm{C}^{-1}\ \mathrm{min}^{-1}]Tt \\ &\quad + [0.683\ \mathrm{GPa}\ \mathrm{min}^{-1}])t \\ &\quad + ([-0.00317\ \mathrm{GPa}\ °\mathrm{C}^{-1}]T + [224.6\ \mathrm{GPa}])\end{aligned} \tag{5}$$

where T is process temperature in °C and t is the number of minutes the sample is heated at or above 480 °C. These empirical fits provide a guideline for anticipating the trade-off in strength and stiffness as a function of time exposed to temperatures >480 °C when engineering a thermal process for HTR40 fibers.

To better characterize the nature of the hypothesized thermally activated strength- and stiffness-loss process, thermogravimetric analysis (TGA) was performed with HTR40 fibers in He atmosphere (3 mg chopped fiber per run). TGA of fibers at a constant heating rate of 100 °C min^{-1} (comparable to what is encountered during CNT growth in the CVD furnace) reveals a sudden change in mass-loss rate beginning at 550 °C (Figure 3b). Similarly, TGA over the course of 60 min at constant temperatures of 400, 500, and 650 °C (Figure 3a) reveal that time-dependent mass loss only occurs at 650 °C.

To verify the observed results were not peculiar to the specific HTR40 product used in most of this study, similar single-fiber tensile tests were performed with heat-treated AS4 fibers as well. Tensile strength (Figure 4b) and tensile stiffness (Figure 4d) for unsized AS4 as received and after heat treatment in He at 480 °C, 580 °C, and 730 °C were found to undergo similar temperature-dependent losses to HTR40, although less severe at temperatures below 600 °C. Thus the observed responses of the HTR40 carbon fibers are not isolated to one specific product and are generally relevant to modern aerospace-grade high-tenacity ex-PAN carbon fibers.

Drawing on these results, it was further hypothesized that this mass loss may be correlated with a loss of HCN, the major byproduct generated from the pyrolysis of poly(acrylonitrile)-derived carbon fibers such as HTR40 and AS4. In-line mass spectrometry with adequate capability to differentiate the release of this from CO (another expected byproduct which has the same mass number as HCN but different mass defect) was not available (noting that a mass spectrometer with a resolution better than ±1 amu would be able to resolve the two). Instead, a surface analysis using Auger spectroscopy was performed to detect changes in the nitrogen-to-carbon ratio present on the

dx.doi.org/10.1021/am4006385 | ACS Appl. Mater. Interfaces 2013, 5, 4892−4903

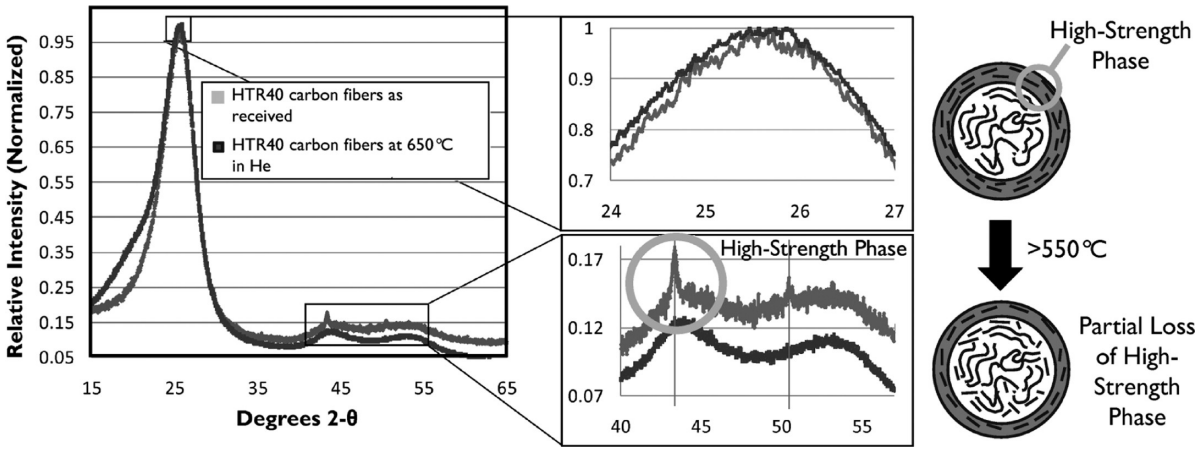

Figure 5. (Left) XRD of HTR40 as received (gray trace) and in situ XRD of HTR40 while being heated in He at 650 °C (black trace) showing the superposition of two graphite phases, one of which (with a larger domain size) disappears upon heat treatment; (right) depiction of hypothesized origin of strength loss in the context of the skin-core model of ex-PAN carbon fibers.

carbon fiber surface: if HCN is volatilized as a result of heat treatment, the carbon fiber would be expected to contain N, and a decrease in its concentration as a result of HCN offgassing should be measurable. Figure 3c shows the C:N ratio measured by Auger spectroscopy of unsized HTR40 fibers as received and after thermal processing in He at 480, 580, and 730 °C. A measurable, temperature-dependent loss of N is clearly observed. Notably, the largest drop in N content occurs between the as-received fibers and the fibers heat-treated at 480 °C, even though strength and (generally) stiffness are preserved at this temperature.

To gain insights about microstructural changes throughout the bulk of the fiber (the interior core), we performed X-ray diffraction (XRD) on unsized HTR40 fibers before and after thermal processing in He at 730 °C (Figure 5). The as-received fibers display a superposition of two phases of graphite—one with a very small domain size (tens of nm, the broad peaks at 44 and 53° 2θ) and one with larger domain sizes (hundreds of nanometers, the sharp peaks at 44 and 53° 2θ and possibly an accentuated feature at 25.7° 2θ). The disappearance of the phase associated with the larger graphite domain sizes upon heat treatment in He at 730 °C, in combination with the chemical changes on the carbon fiber surface observed by Auger spectroscopy, suggests that a microstructural rearrangement within the carbon fiber occurs beginning at ~550 °C, wherein the minority strength-bearing phase (the highly oriented surface shell of the fiber with large domains) restructures, leaving a weaker phase (the less-oriented interior core of the fiber with smaller domains) as the dominant load-bearing continuity.

Thus it appears there exists an inherent mechanochemical coupling of fiber strength and compositional aspects of the fiber's microstructure. Extending this, one of the most critical dimensions in the parameter space of carbon fiber manufacturing is the role of tension during various phases of production—in fact, in the case of most ex-PAN carbon fibers, the fiber is tensioned to significant proportions of its tensile strength during production. Tensioning is an especially important aspect of imparting high tensile strength to high-performance carbon fibers. Not only do chemical changes affect the mechanical properties of carbon fibers, but mechanical forces can be used to direct the chemical evolution of the fiber microstructure.

3.3. CVD Growth of CNTs on Carbon Fibers Under Tension. One critical difference between the environment in which the carbon fibers studied are manufactured and the environment of the CVD system used is the absence of applied tension when heated. In light of the observed mechanochemical coupling of strength and stiffness with microstructural reconfiguration at elevated temperatures, we hypothesized that introducing tension during CNT growth on the already-manufactured fibers analogous to the conditions encountered during manufacture could help preserve fiber tensile properties. Tension was applied to single carbon fibers using a specially designed all-graphite single-fiber tensioning frame (see the Supporting Information). The tension applied to a fiber can be expressed as a proportion of the fiber tensile strength, $\bar{\sigma}$. We set the dimensionless ratio $\bar{\Xi}$ equal to the tension applied to a fiber during CVD normalized by the mean tensile strength measured for unmodified, unprocessed fibers of the same type as determined by prior single-fiber tensile tests. Single-fiber loadings of $\bar{\Xi}$ = 0.12, $\bar{\Xi}$ = 0.45, and $\bar{\Xi}$ = 0.75 were investigated. At tensions of $\bar{\Xi}$ = 0.75, fewer than one in ten fibers survived thermal processing, and so this level of tension was not studied in depth (in fact, this level of tension likely serves more as a mechanism for selecting out the highest strength fibers from a set of fibers rather than a method for tensioning the fibers).

Figure 6 shows Weibull distributions calculated from tensile tests performed on unsized HTR40 fibers as received and after heat treatment at 730 °C (at or above 480 °C for 18 min) with $\bar{\Xi}$ = 0.12 and $\bar{\Xi}$ = 0.45 (see the Supporting Information for tabular data). The application of a low level of tension ($\bar{\Xi}$ = 0.12) was found not only to preserve carbon fiber tensile stiffness and strength upon thermal processing at 730 °C but possibly also to enhance tensile strength. Similarly, CVD growth of CNTs employing ethylene and hydrogen at 730 °C on h-PSMA/alumina/Fe^{3+}-coated HTR40 fibers tensioned to $\bar{\Xi}$ = 0.12 resulted in CNT growth and simultaneous preservation of fiber tensile strength and modulus. Interestingly, however, the higher level of tension ($\bar{\Xi}$ = 0.45) resulted in ~10% loss in tensile strength over as-received fibers, although this is still a 20–25% improvement in strength retention compared with untensioned thermal processing of fibers.

In conclusion, application of a low level of tension is a viable strategy for preserving fiber strength and stiffness during CNT growth on carbon fibers. While here we retensioned aerospace-grade carbon fibers postmanufacture, the CNT growth process

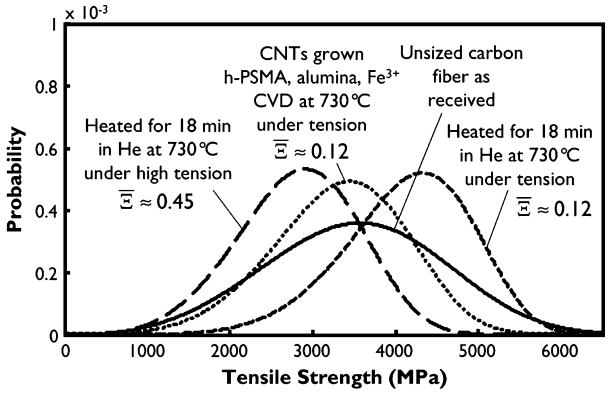

Figure 6. Weibull distributions showing the tensile strength of HTR40 carbon fibers tensioned in situ during heat treatment in He at 730 °C and during CVD growth of CNTs showing preservation of fiber strength is achieved through application of a tension of approximately 12% of fiber tensile strength ($\bar{\Xi} = 0.12$).

could also be integrated into current manufacturing processes, which already put the fibers under varying degrees of tension.

3.4. CVD Growth of CNTs on Carbon Fibers Below Strength-Loss Threshold Temperature. On the basis of the observation of a strength- and stiffness-loss process activation temperature of ~550 °C for HTR40 fibers (and slightly higher for AS4 fibers), it was hypothesized that if it were possible to grow CNTs below 550 °C, tension would not be needed to preserve carbon fiber tensile properties. Here, the method of low-temperature CNT growth employing carbon dioxide and acetylene described by Magrez et al.[41] in combination with Fe^{3+}-loaded K-PSMA is used to grow CNTs on HTR40 carbon fibers at 480 °C—well below the critical temperature threshold of 550 °C. Figure 7 summarizes tensile tests performed on unsized HTR40 and CVD-processed Fe^{3+}/K-PSMA-coated HTR40 fibers (see also Supporting Information). Remarkably, CNTs were obtained and no changes in tensile strength or tensile modulus are observed, despite the absence of applied tension.

In summary, CNT growth can be achieved on high-performance carbon fibers without resulting in degradation of fiber tensile properties without tensioning.

4. CONCLUSIONS

The origins of strength and stiffness degradation due to CVD growth of CNTs on advanced ex-PAN carbon fibers was characterized at the single-fiber level. We find that the origins of this strength loss arise from thermally activated mechanochemical changes in the fiber microstructure when heated in an untensioned state above a fiber-product-specific critical threshold temperature (~550 °C for the HTR40 fibers examined in this study and closer to ~600 °C for AS4 fibers). Above this threshold temperature, chemical and microstructural changes are observed. Strength and stiffness loss can be mitigated through application of tension to the fiber during CNT growth when employing CVD processes above this temperature. We hypothesize the application of tension mechanically guides the evolution of these chemical and microstructural changes, perhaps by invoking alignment and thus better overlap of graphitic ribbons within the outer skins of the fibers, thereby actively increasing fiber modulus and strength in a compensatory fashion. We further hypothesize that, upon cooling, the tension-invoked microstructural state is kinetically trapped as-is and only when heated above the critical threshold temperature will restructuring resume, thus providing

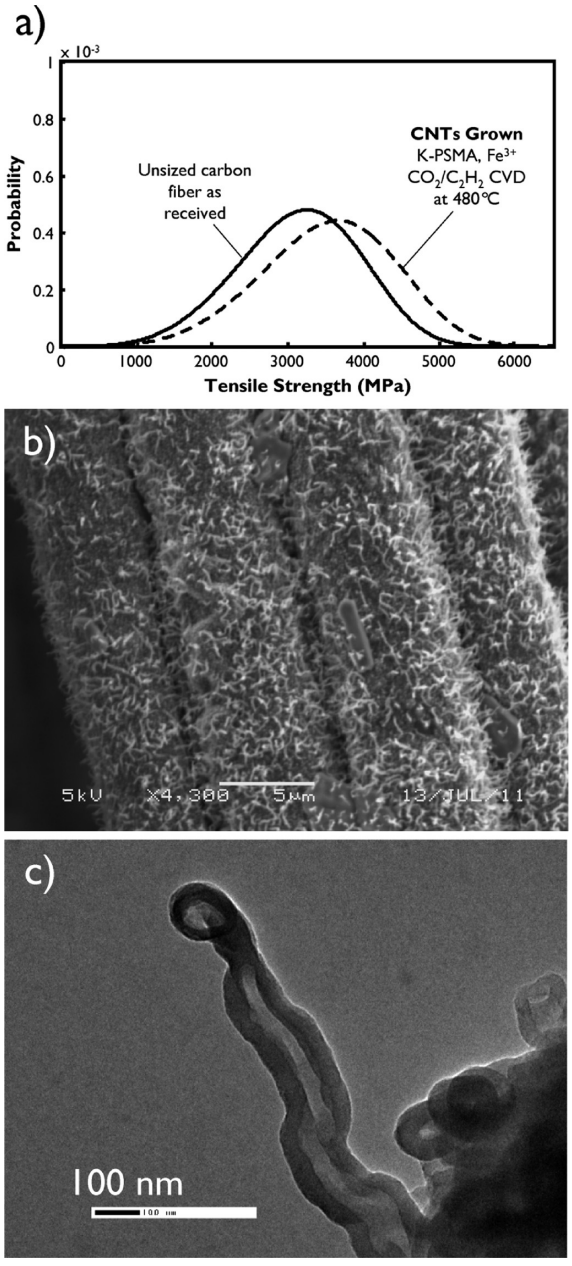

Figure 7. (a) Weibull distribution of tensile strength of carbon fibers following CVD growth of CNTs employing CO_2/C_2H_2 at 480 °C showing preservation of fiber strength; (b) SEM image of CNTs grown on carbon fibers coated with K-PSMA and Fe^{3+} with CO_2/C_2H_2 process at 480 °C; (c) TEM image of large-diameter multiwalled CNT extending off carbon fiber, resulting from strength-preserving CO_2/C_2H_2 process performed at 480 °C.

an avenue for preserving tensile properties. We demonstrate that it is in fact possible to preserve fiber strength and stiffness by tensioning carbon fibers during CVD growth at temperatures in excess of 700 °C. We also demonstrate that fiber strength and stiffness can be preserved by performing CVD below the fiber's strength-loss threshold temperature using a process such as low-temperature oxidative dehydrogenation growth. This approach may be more amenable to substrates such as weaves that cannot be tensioned easily. Coatings approaches for facilitating low-temperature growth and CNT alignment that do not require chemical etching of the carbon fiber surface have also been demonstrated and shown effective at producing fibers suitable for

dx.doi.org/10.1021/am4006385 | ACS Appl. Mater. Interfaces 2013, 5, 4892−4903

use in advanced composites applications. This study provides, for the first time, viable pathways for growing CNTs on carbon fibers suitable for advanced composites applications without compromising in-plane properties. Hierarchical carbon fibers produced through these approaches may also find application as electrodes for batteries, supercapacitors, and structures that double as energy-storing devices. We note that while unsized fibers such as those used in this study may provide a more ideal surface for the application of functional coatings than sized fibers, current commercial manufacture of carbon fibers relies on sizings for many aspects of processing and handling, and many resin systems leverage carbon fiber sizings for fiber-matrix bonding. This said, the approaches demonstrated in this work could easily be extended to sized fibers by appropriately tailoring the polyelectrolyte and sizing chemistries to allow for noncovalent functionalization of sized carbon fiber surfaces. Alternatively, sized fibers could be desized (i.e., the sizing could be removed) prior to CNT growth via solvent treatment or thermal treatment in air or inert atmosphere. Hierarchical carbon fibers offer numerous processing advantages over sized carbon fibers, however, including the ability to wick resins into the fiber via capillarity-driven wetting as well as greatly enhanced interfacial area for bond formation, suggesting that hierarchical carbon fibers such as those produced in this work may ultimately displace the need for sizings altogether.

■ ASSOCIATED CONTENT

Supporting Information

Detailed experimental procedures, engineering diagrams for single-fiber processing apparatus used in this work, and tabular data of single-fiber tensile tests performed. This material is available free of charge via the Internet at http://pubs.acs.org.

■ AUTHOR INFORMATION

Corresponding Author

*E-mail: ssteiner@alum.mit.edu. Phone: +1 (617) 324-3400.

Author Contributions

The manuscript was written through contributions of all authors. All authors have given approval to the final version of the manuscript.

Notes

The authors declare no competing financial interest.

■ ACKNOWLEDGMENTS

The authors thank Dr. Roberto Guzmán de Villoria for his assistance in performing tensile tests conducted in this work, Akira Kudo for his assistance in acquiring TEM images, Dr. Woo Sik Kim for his assistance with alkoxide-derived alumina coating development, Megan Tsai and Dr. Kyoko Ishiguro for their assistance in carbon fiber substrate preparation, Dr. Scott Speakman for his assistance in performing X-ray diffraction, Libby Shaw for her expertise in conducting Auger spectroscopy, and Nathan Brei for his contributions to the all-graphite tensioning frame. The authors also thank TohoTenax Corporation for valuable technical discussions. This work was supported by Boeing, EADS, Embraer, Lockheed Martin, Saab AB, Hexcel, TohoTenax, and Composite Systems Technology through MIT's Nano-Engineered Composite aerospace STructures (NECST) Consortium. This work was supported (in part) by the National Science Foundation under Grant No. DMR-10007793 (NSF-EPSRC Materials World Network) and (in part) by the U.S. Army Research Office under contract W911NF-07-D-0004. This work made use of the MIT MRSEC Shared Experimental Facilities in the MIT Center for Materials Science and Engineering supported by the National Science Foundation under Award Number DMR-0819762.

■ REFERENCES

(1) Baker, A.; Dutton, S.; Kelly, D. *Composite Materials for Aircraft Structures*, 2nd ed.; American Institute of Aeronautics and Astronautics: Reston, VA, 2004.

(2) Gardiner, G. Lightning Strike Protection for Composite Structures. *High-Performance Composites* [Online], Jul 1, **2006**. http://www.compositesworld.com/articles/lightning-strike-protection-for-composite-structures (accessed Nov 18, 2012).

(3) Gojny, F. H.; Wichmann, M. H. G.; Köpke, U.; Fiedler, B.; Schulte, K. *Compos. Sci. Technol.* **2004**, *64*, 2363−2371.

(4) Qiu, J.; Zhang, C.; Wang, B.; Liang, R. *Nanotechnology* **2007**, *18*, 275708−275719.

(5) Bekyarova, E.; Thostenson, E. T.; Yu, A.; Kim, H.; Gao, J.; Tang, J.; Hahn, H. T.; Chou, T.-W.; Itkis, M. E.; Haddon, R. C. *Langmuir* **2007**, *23*, 3970−3974.

(6) Bekyarova, E.; Thostenson, E. T.; Yu, A.; Itkis, M. E.; Fakhrutdinov, D.; Chou, T.-W.; Haddon, R. C. *J. Phys. Chem. C* **2007**, *111*, 17865−17871.

(7) Zhua, J.; Imamb, A.; Cranec, R.; Lozanod, K.; Khabasheskue, V. N.; Barreraf, E. V. *Compos. Sci. Technol.* **2007**, *67*, 1509−1517.

(8) Dzenis, Y. *Science* **2008**, *319*, 419−420.

(9) Adhikari, K.; Hubert, P.; Simard, B.; Johnston, A. Effect of the Localized Application of SWNT Modified Epoxy on the Interlaminar Shear Strength of Carbon Fiber Laminates. In *47th AIAA Structures, Dynamics, and Materials Conference Proceedings*; Newport, RI, May 1−4, 2006 ; American Institute of Aeronautics and Astronautics: Reston, VA, 2006.

(10) Thakre, P. R.; Zhu, J.; Barrera, E. V. Processing and Characterization of Epoxy-SWCNT-Woven Fabric Composites. In *47th AIAA Structures, Dynamics, and Materials Conference Proceedings*; Newport, RI, May 1−4, 2006; American Institute of Aeronautics and Astronautics: Reston, VA, 2006.

(11) Garcia, E. J.; Wardle, B. L.; Hart, A. J. *Composites, Part A* **2008**, *39*, 1065−1070.

(12) Veedu, V. P.; Cao, A.; Li, X.; Ma, K.; Soldano, C.; Kar, S.; Ajayan, P. M.; Ghasemi-Nejhad, M. N. *Nat. Mater.* **2006**, *5*, 457−462.

(13) Qian, H.; Greenhalgh, E. S.; Shaffer, M. S. P.; Bismarck, A. *J. Mater. Chem.* **2010**, *20*, 4751−4762.

(14) Wicks, S. S.; Guzmán de Villoria, R.; Wardle, B. L. *Compos. Sci. Technol.* **2010**, *70*, 20−28.

(15) Garcia, E. J.; Wardle, B. L.; Hart, A. J.; Yamamoto, N. *Compos. Sci. Technol.* **2008**, *68*, 2034−2041.

(16) Wicks, S. S.; Guzmán de Villoria, R.; Barber, D. M.; Wardle, B. L. Fracture Toughness of a Woven Advanced Composite Reinforced with In Situ-Grown Aligned Carbon Nanotubes. In *Proceedings of the 50th AIAA Structures, Structural Dynamics, and Materials Conference*; Palm Springs, CA, May 4−7, 2009 ; American Institute of Aeronautics and Astronautics: Reston, VA, 2009.

(17) Garcia, E. J.; Hart, A. J.; Wardle, B. L. *AIAA J.* **2008**, *46*, 1405−1412.

(18) Garcia, E. J.; Hart, A. J.; Wardle, B. L.; Slocum, A. H. *Nanotechnology* **2007**, *18*, 165602/1−165602/11.

(19) Yamamoto, N.; Hart, A. J.; Garcia, E. J.; Wicks, S.; Duong, H. M.; Slocum, A. H.; Wardle, B. L. *Carbon* **2009**, *47*, 551−556.

(20) Blanco, J.; Garcia, E. J.; Guzmán de Villoria, R.; Wardle, B. L. *J. Compos. Mater.* **2009**, *43*, 825−842.

(21) Downs, W. B.; Baker, R. T. K. *Carbon* **1991**, *29*, 1173−1179.

(22) Simon, R. A. *Silicon Carbide Whiskers on Carbon Fibers to Improve Resin Adhesion*; Technical Report for the Naval Ordinance Lab, White Oak, MD; Defense Technical Information Center: Ft. Belvoir, VA, 1973.

(23) Garcia, R. *Methods of Improving the Matrix Dominated Performance of Composite Structures: A Technical Review*; Technical Report for the Naval Air Development Center Aircraft and Crew Systems Technology

Directorate, Warminster, PA; Defense Technical Information Center: Ft. Belvoir, VA, 1983.
(24) Garcia, R.; Evans, R. E.; Palmer, R. J. *ASTM Spec. Tech. Publ.* **1987**, *937*, 397−412.
(25) Yamashita, S.; Hatta, H.; Takei, T.; Sugano, T. *J. Compos. Mater.* **1992**, *26*, 1254−68.
(26) Wang, W. X.; Takao, Y.; Matsubara, T.; Kim, H. S. *Compos. Sci. Technol.* **2002**, *62*, 767−774.
(27) Downs, W. B.; Baker, R. T. K. *J. Mater. Res.* **1995**, *10*, 625−633.
(28) Kepple, K. L.; Sanborn, G. P.; Lacasse, P. A.; Gruenberg, K. M.; Ready, W. J. *Carbon* **2008**, *46*, 2026−2033.
(29) Qian, H.; Bismarck, A.; Greenhalgh, E. S.; Kalinka, G.; Shaffer, M. S. P. *Chem. Mater.* **2008**, *20*, 1862−1869.
(30) Sager, R. J.; Klein, P. J.; Lagoudas, D. C.; Zhang, Q.; Liu, J.; Dai, L.; Baur, J. W. *Compos. Sci. Technol.* **2009**, *69*, 898−904.
(31) Mathur, R. B.; Chatterjee, S.; Singh, B. P. *Compos. Sci. Technol.* **2008**, *68*, 1608−1615.
(32) Zhang, Q.; Liu, J.; Sager, R.; Dai, L.; Baur, J. *Compos. Sci. Technol.* **2009**, *69*, 594−601.
(33) Cesano, F.; Bertarione, S.; Scarano, D.; Zecchina, A. *Chem. Mater.* **2005**, *17*, 5119−5123.
(34) Chen, L.-H.; AuBuchon, J. F.; Chen, I.-C.; Daraio, C.; Ye, X.-R.; Gapin, A.; Jin, S.; Wang, C. M. *Appl. Phys. Lett.* **2006**, *88*, 033103.
(35) Qu, L.; Zhao, Y.; Dai, L. *Small* **2006**, *2*, 1052−1059.
(36) He, X.; Zhang, F.; Wang, R.; Liu, W. *Carbon* **2007**, *45*, 2559−2563.
(37) Li, J.; Steigerwalt, E. S.; Sambandam, S.; Lu, W.; Lukehart, C. M. *Chem. Mater.* **2007**, *19*, 6001−6006.
(38) Laachachi, A.; Vivet, A.; Nouet, G.; Doudou, B. B.; Poilâne, C.; Chen, J.; Bai, J. B.; Ayachi, M. H. *Mater. Lett.* **2008**, *62*, 394−397.
(39) Fan, Z.; Wu, C.; Chen, J. *Carbon* **2008**, *46*, 365−389.
(40) Kim, H. S.; Kim, B.; Lee, B.; Chung, H.; Lee, C. J.; Yoon, H. G.; Kim, W. *J. Phys. Chem. C Lett.* **2009**, *113*, 17983−17988.
(41) Magrez, A.; Seo, J. W.; Smajda, R.; Korbely, B.; Andresen, J. C.; Mionic, M.; Casimirius, S.; Forro, L. *ACS Nano* **2010**, *4*, 3702−3708.
(42) Stroock, A. D.; Kane, R. S.; Weck, M.; Metallo, S. J.; Whitesides, G. M. *Langmuir* **2003**, *19*, 2466−2472.
(43) Baumann, T. F.; Gash, A. E.; Chinn, S. C.; Sawvel, A. M.; Maxwell, R. S.; Satcher, J. H., Jr. *Chem. Mater.* **2005**, *17*, 395−401.
(44) *Standard Test Method for Tensile Strength and Young's Modulus for High-Modulus Single-Filament Materials*, D3379-75; ASTM International: West Conshohocken, PA, 1989.
(45) *Carbon Fibre—Determination of the Tensile Properties of Single-Filament Specimens*, ISO 1156; International Standards Organization: Geneva, Switzerland, 1996.
(46) Steiner III, S. A. Carbon Nanotube Growth on Challenging Substrates: Applications for Carbon-Fiber Composites. *Ph.D. Thesis*, Massachusetts Institute of Technology, Cambridge, MA, 2011.
(47) Dresselhaus, M. S.; Dresselhaus, G.; Sugihara, K.; Spain, I. L.; Goldberg, H. A. *Graphite Fibers and Filaments*; Springer-Verlag, 1988.
(48) Hofmann, S.; Blume, R.; Wirth, C. T.; Cantoro, M.; Sharma, R.; Ducati, C.; Haevecker, M.; Zafeiratos, S.; Schnoerch, P.; Oestereich, A.; Teschner, D.; Albrecht, M.; Knop-Gericke, A.; Schloegl, R.; Robertson, J. *J. Phys. Chem. C* **2009**, *113*, 1648.
(49) Hofmann, S.; Sharma, R.; Ducati, C.; Du, G.; Mattevi, C.; Cepek, C.; Cantoro, M.; Pisana, S.; Parvez, A.; Cervantes-Sodi, F.; Ferrari, A. C.; Dunin-Borkowski, R.; Lizzit, S.; Petaccia, L.; Goldoni, A.; Robertson, J. *Nano Lett.* **2007**, *7*, 602−608.
(50) Steiner, S. A., III; Li, R.; Guzman de Villoria, R.; Tsai, M. S.; Wardle, B. L. Methods for Growing Carbon Nanotubes on Carbon Fibers that Preserve Fiber Tensile Strength. In *Proceedings of the 51st AIAA Structures, Structural Dynamics, and Materials (SDM) Conference*; Orlando, FL, April 12−15, 2010; American Insitute of Aeronautics and Astronautics: Reston, VA, 2010.
(51) Carrillo, A.; Swartz, J. A.; Gamba, J. M.; Kane, R. S.; Chakrapani, N.; Wei, B.; Ajayan, P. M. *Nano Lett.* **2003**, *3*, 1437−1440.
(52) Harlow, E. G.; Phoenix, L. *J. Compos. Mater.* **1978**, *12*, 195−214.
(53) Saito, K.; Ogawa, H. Studies on Thermal Oxidative Stability of Carbon Fiber. In *Proceedings of the 31st International SAMPE Symposium*; Las Vegas, NV, April 7−10, 1986; Society for the Advancement of Material and Process Engineering: Covina, CA, 1986.